Pulsed liquid microjet for microsurgery

D. A. Fletcher[a)]
E. L. Ginzton Laboratory, Stanford University, Stanford, California 94305

D. V. Palanker
Hansen Experimental Physics Laboratory, Stanford University, Stanford, California 94305 and Department of Ophthalmology, School of Medicine, Stanford University, Stanford, California 94305

(Received 6 October 2000; accepted for publication 30 January 2001)

The precision of soft tissue dissection with pulsed lasers in liquid media is typically limited by collateral damage from vapor bubbles created during energy deposition. We present an alternative technique for creating incisions using a pulsed liquid microjet driven by an electric discharge-induced vapor bubble generated inside a micronozzle. We use this technique to create a pulsed jet 30 μm in diameter with a peak velocity of 90 m/s and total ejected volume on the order of 100 pl. Incision tests on a polyacrylamide gel simulating soft tissue show that the width of the cut is comparable to the diameter of the micronozzle and that collateral damage is significantly less than that produced by a vapor bubble not confined by the nozzle. © *2001 American Institute of Physics.* [DOI: 10.1063/1.1357452]

Lasers are widely used in surgical procedures for precise dissection of soft tissue in fluid media. Energy deposition results from either absorption of laser radiation or from dielectric breakdown in the focal area of a short-pulsed laser beam.[1–3] In liquid media, energy deposition leads to explosive evaporation of fluid at the focus and is accompanied by formation of a vapor bubble that can cause substantial collateral damage during its growth and collapse.[4,5] In cardiovascular surgery, expanding vapor bubbles can stretch the walls of blood vessels during laser angioplasty, causing restenosis of the damaged vessel walls.[6] Collapsing vapor bubbles are the main source of collateral damage in intraocular surgical applications of focused or fiber-delivered pulsed lasers and pulsed electric discharges.[1,7]

Liquid jets are an alternative to lasers for cutting soft tissue in which energy is deposited mainly in the direction of the flow. Continuous water jets powered by compressed air have been used for cutting neuronal connections in nervous tissue slices as well as in laparascopic surgery of the liver.[8,9] While effective for an air-tissue interface, the continuous flow of fluid does not allow precise control of cutting depth when applied in liquid media. Acoustic excitation or thermal bubble expansion for printing applications can generate pulsed jets with velocities of 20–30 m/s in air but do not operate in water.[10,11] For microsurgical and biological applications, a short-pulsed liquid jet capable of making incisions fewer than 50 μm across is needed for precise dissection of soft tissue in liquid media.

In this letter, we describe a pulsed liquid microjet driven by an electric discharge-induced vapor bubble inside a micronozzle. The three-dimensional expansion of the confined vapor bubble, which can cause collateral damage to surrounding tissue in pulsed laser microsurgery, is used to drive a one-dimensional liquid jet through the micronozzle. We demonstrate a pulsed jet 30 μm in diameter with a peak velocity of 90 m/s and ejected volume on the order of 100 pl. Incision tests on a polyacrylamide gel simulating soft tissue show that gel is removed within a region comparable in diameter to the liquid jet.

The device consists of a high-voltage electrode, tapered micronozzle, and exit hole as diagramed in Fig. 1. The tapered micronozzle is formed from a borosilicate glass pipette heated by a CO_2 laser and drawn in a pipette puller. The exit aperture is polished and further heated under a microscope to reflow the glass to an exit hole diameter of 30 μm. The nozzle is filled with a saline solution and fixed over a high-voltage electrode approximately 3 mm from the exit aperture. The electrode consists of a 25 μm diameter tungsten wire surrounded by a quartz insulator and grounded metal sheath. Ionic conduction through the saline solution connects the electrode tip with the sheath. When a voltage on the order of 1 kV is applied to the electrode, the field at the tip accelerates electrons towards the anode, creating plasma streamers with temperatures of approximation 10 000 K.[12–14] Heat deposited in the surrounding saline during the 0.5 μs discharge causes explosive growth of a vapor bubble. In a constant pressure environment, bubble expansion and col-

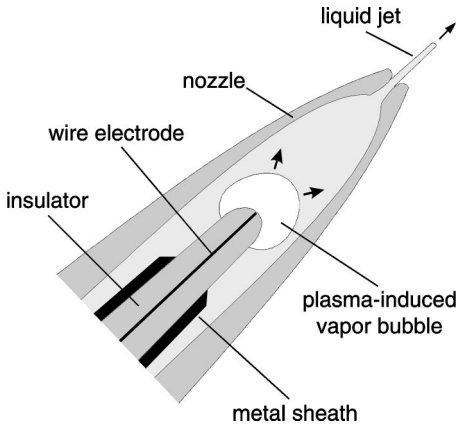

FIG. 1. Schematic diagram of the pulsed liquid microjet driven by expansion of a vapor bubble created by a submicrosecond high-voltage discharge.

a)Electronic mail: dan.fletcher@stanford.edu

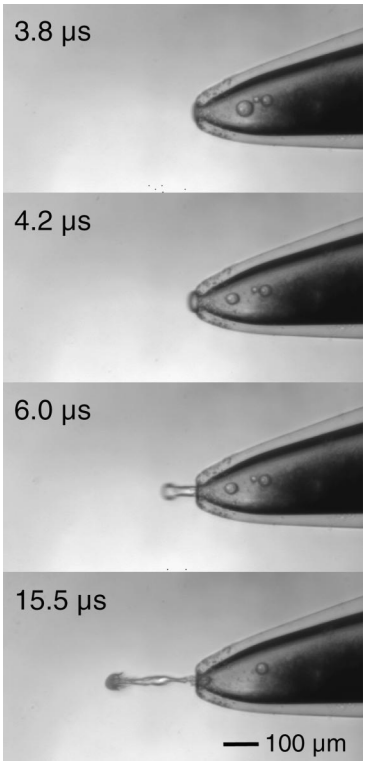

FIG. 2. Time sequence of saline ejection into oil from a 30 μm nozzle driven by a 280 μJ discharge. Times noted on each frame correspond to delays after the electrical discharge.

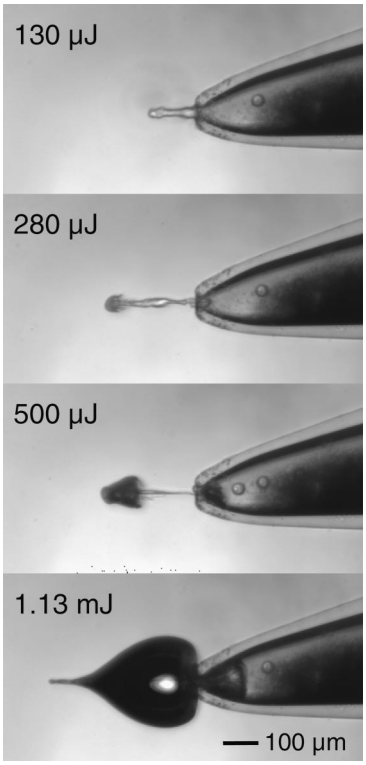

FIG. 3. Saline ejection into oil from a 30 μm nozzle driven by increasing discharge energies. Each frame is taken 15.5 μs after the electrical discharge. Note the appearance of hydrodynamic cavitation bubbles at high energies.

lapse at the electrode tip follows a model proposed by Rayleigh.[15] Inside the micronozzle, the expanding bubble pushes a small volume of liquid through the exit hole.

Time-resolved imaging of fluid ejection by the pulsed liquid microjet is performed on an inverted microscope using shadow photography with 0.3 μs flash from a light-emitting diode (LED). The micronozzle filled with saline is submerged in oil to provide optical contrast to the liquid ejected by the microjet. We trigger the high-voltage electric discharge and flash the LED after a time controlled with a delay generator. The image is collected by a liquid nitrogen cooled charge coupled device camera with 512×512 pixels (TKB-1-VISAR, Princeton Instruments, Inc.). We extract information on ejection velocity, volume, and dynamics from time sequences of the ejection process. Though each image is taken of a different pulse, the ejection is stable and reproducible and can be considered to represent the time evolution after a single pulse. Pulse-to-pulse variations in ejection size at a given time were observed to be less than 10%.

Figure 2 shows ejection of a single pulse from a nozzle with a 30 μm diameter exit hole. An energy of 280 μJ is deposited at time zero during the 0.5 μs discharge, and delay times after discharge are shown in each frame. The velocity of the fluid stream ejected from the nozzle averaged between the first two frames in Fig. 2 is 63 m/s, slowing to 25 m/s between the last two frames. Since the saline solution does not mix with oil, the ejected fluid volume and trajectory can be determined from the images. With a 280 μJ discharge, approximately 50 pl of saline is ejected a distance of 300 μm during a single pulse. As the vapor bubble driving the microjet collapses, the ejected volume is replaced by fluid drawn back into the nozzle or by small bubbles remaining after collapse of the vapor bubble. Ejection speed and repeatability is reduced when the exit hole is obstructed by gas bubbles. Small volumes of oil drawn into the nozzle during previous pulses can be seen in Fig. 2.

The kinetic energy of the ejected fluid can be estimated from the volume of the ejected fluid and an average ejection velocity. Based on a maximum velocity of 63 m/s, the average ejection velocity is calculated to be 41 m/s assuming the bubble expands according to the Rayleigh equation within the micronozzle.[16] The kinetic energy required to eject 50 pl of fluid at the average velocity is approximately 40 nJ, nearly four orders of magnitude smaller than the discharge energy. Experiments with the unconfined electrode in saline show that about 10% of the discharge energy is converted into vapor bubble expansion.[7] The vapor bubble within the micronozzle is smaller than in a free liquid due to the rise in pressure inside. Energy losses at the nozzle exit and at the joint between the nozzle and electrode further reduce the conversion efficiency of the discharge energy into kinetic energy of the ejected flow.

As discharge energy is increased, ejection velocities and volumes increase, and hydrodynamic cavitation bubbles appear at the exit hole. Figure 3 shows ejection images at several discharge energies taken at a constant delay time of 15.5 μs after discharge. For a discharge energy of 1.13 mJ, approximately 200 pl of fluid is ejected at an initial speed of nearly 90 m/s. The cavitation bubbles observed in Fig. 3 are produced when the tensile stress on cavitation nuclei overcomes surface tension and inertial forces. Using the Bernoulli equation, we estimate that a tensile stress of 1.9 MPa is generated in the 63 m/s flow and is sufficient to cause

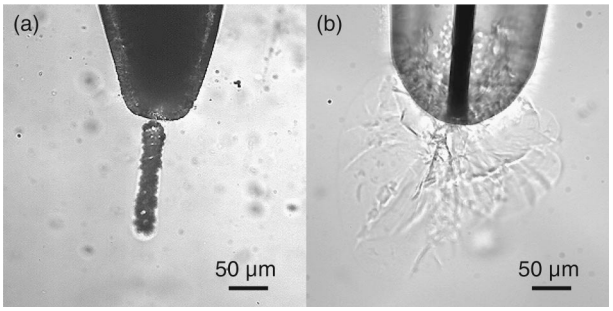

FIG. 4. Comparison of incisions in a polyacrylamide gel after a series of discharges from (a) the pulsed liquid microjet at 1.13 mJ/pulse and (b) the direct application of the plasma-induced vapor bubble at 0.14 mJ/pulse.

hydrodynamic cavitation at the nozzle exit. This tensile stress is a factor of 2 larger than that observed for thermoelastically induced cavitation,[17,18] due in part to differences in geometry and flow dynamics. An increase in discharge energy beyond the cavitation threshold results in a rise in ejection velocity and in formation of larger cavitation bubbles that originate further inside the nozzle, as shown in Fig. 3. Both low- and high-energy discharge tests were also conducted in saline solution rather than oil, and results showed cavitation inception at similar energies.

We tested the pulsed liquid microjet's cutting characteristics by placing it in contact with the surface of a 10% polyacrylamide gel (80% water) submerged in saline. Figure 4(a) shows a cut approximately 35 μm in diameter and 150 μm in depth created in the gel after multiple pulses of the microjet with discharge energy of 1.1 mJ/pulse. The cut diameter is comparable to the diameter of the nozzle exit hole, and the aspect ratio of the incision is nearly 5:1. No collateral damage beyond the diameter of the incision is observed. For comparison, the same gel is shown in Fig. 4(b) after direct application of a series of electric discharges at 0.14 mJ/pulse to the surface of the material. Fragmentation from the vapor bubble extends radially approximately 200 μm beyond the electrode, indicating that the width of the damage zone in this mode is about ten times larger than that achieved with the jet. Note that the energy deposited into the gel by the microjet is more than a factor of 100 smaller than that deposited by the vapor bubble. This ratio is similar to the volume ratio of fragmented material created by the two methods shown in Fig. 4. Although transparent polyacrylamide gel is a convenient material for study of jet interaction with soft tissue and for imaging incisions and associated damage zones, further experimentation is required to evaluate the efficacy of the pulsed liquid microjet for procedures involving particular biological tissues.

Variations in nozzle geometry and discharge energy can alter the ejection velocity, volume, and dynamics of the jet. For a given discharge energy, an increase in nozzle exit diameter is observed to reduce ejection speed and raise the hydrodynamic cavitation threshold energy. Similarly, a reduction in exit diameter is expected to decrease the flow diameter and lower the cavitation threshold energy. The discharge energy is currently limited by structural failure of the borosilicate glass micronozzle to discharge energies smaller than approximately 1.5 mJ/pulse.

In conclusion, we have demonstrated a pulsed liquid microjet driven by an electric discharge-induced vapor bubble. Ejection velocities of 90 m/s and volumes on the order of 100 pl are observed for 30 μm diameter jets. The diameter of the incision created by the pulsed liquid microjet is significantly smaller than the fragmentation zone resulting from direct application of the vapor bubble for similar incision depths. The device enables tissue fragmentation with a well-defined incision width as well as ejection of a precise volume of liquid. Such advantages may be useful in revascularization applications, transluminal and transcutaneous drug delivery, and microsurgical tissue dissection.

This work was funded in part by the Stanford University Incentive Fund. The authors thank Professor Rox Anderson from Wellman Laboratories of Photomedicine, Harvard Medical School and Jasen Miller from Stanford Medical School for helpful discussions of the concept and its possible applications. The authors also thank Professor Alfred Vogel for his comments and advice.

[1] A. Vogel, P. Schweiger, A. Frieser, M. N. Asiyo, and R. Birngruber, IEEE J. Quantum Electron. **26**, 2240 (1990).
[2] D. Palanker, I. Turovets, and A. Lewis, Lasers Surg. Med. **21**, 294 (1997).
[3] T. G. V. Leeuwen, E. D. Jansen, M. Motamedi, A. J. Welch, and C. Borst, IEEE J. Quantum Electron. **30**, 1339 (1994).
[4] A. Vogel, W. Lauterborn, and R. Timm, J. Fluid Mech. **206**, 299 (1989).
[5] A. Philipp and W. Lauterborn, J. Fluid Mech. **361**, 75 (1998).
[6] T. G. Vanleeuwen, L. Vanerven, J. H. Meertens, M. Motamedi, M. J. Post, and C. Borst, J. Am. Coll. Cardiol. **19**, 1610 (1992).
[7] D. Palanker, I. Turovets, and A. Lewis, J. Appl. Phys. **81**, 7673 (1997).
[8] E.-J. Speckmann, R. Kohling, A. Lucke, H. Straub, W. Wittkowski, C. E. Elger, M. Wiemann, and D. Bingmann, J. Neurosci. Methods **82**, 53 (1998).
[9] H. G. Rau, G. Meyer, T. U. Cohnert, H. M. Schardey, K. Jauch, and F. W. Schildberg, Surgical Endoscopy-Ultrasound and Interventional Techniques **9**, 1009 (1995).
[10] G. L. Fillmore, IEEE Trans. Ind. Appl. **19**, 1098 (1983).
[11] P.-H. Chen, W.-C. Chen, and S.-H. Chang, Int. J. Mech. Sci. **39**, 683 (1997).
[12] P. A. Barnes and K. E. Rieckhoff, Appl. Phys. Lett. **13**, 282 (1968).
[13] H. M. Jones and E. E. Kunhardt, J. Appl. Phys. **77**, 795 (1995).
[14] H. M. Jones and E. E. Kunhardt, J. Appl. Phys. **78**, 3308 (1995).
[15] F. R. Young, *Cavitation* (McGraw-Hill, London, 1989).
[16] C. E. Brennen, *Cavitation and Bubble Dynamics* (Oxford University Press, New York, 1995).
[17] S. L. Jacques, G. Gofstein, and R. S. Dingus, Proc. SPIE **1646**, 284 (1992).
[18] G. Paltauf, E. Reichel, and H. Schmidt-Kloiber, Proc. SPIE **1646**, 343 (1992).